Title

A Convex Modular Modelling (CMM) framework for developing thermodynamically consistent constitutive models

Authors

Stephen K. Suryasentana[1]

Guy T. Houlsby[2]

Affiliations

[1] Department of Civil and Environmental Engineering, University of Strathclyde, Glasgow, UK

[2] Professor Emeritus, Department of Engineering Science, University of Oxford, Oxford, UK

Corresponding author information

Stephen Suryasentana

stephen.suryasentana@strath.ac.uk

Abstract

This paper presents a theoretical framework termed the convex modular modelling (CMM) framework, which provides a convenient and expedient approach for constructing thermodynamically consistent constitutive models. This paper demonstrates how the CMM framework can be used to build increasingly complex constitutive models by mixing and matching re-usable components from a library of convex base functions in a systematic manner. It also describes the use of the modified LogSumExp (MLSE) function as a general and smooth approximation to the pointwise maximum function for any yield function (e.g. the Mohr-Coulomb/Tresca yield function). The MLSE function is then used to develop several new yield functions such as a convex and smooth approximation of the Matsuoka-Nakai yield function, a generalised polygonal yield function and a ‘Reuleaux triangle’-shaped yield function. As CMM is simple to use, it potentially offers a more accessible path for constitutive modellers to take advantage of the hyperplasticity framework to develop robust constitutive models.

Keywords

Plasticity, constitutive modelling

Highlights

- It is challenging to develop increasingly complex constitutive models while ensuring that the models are thermodynamically consistent.
- The paper describes a theoretical framework termed the convex modular modelling (CMM) framework, which provides a convenient and expedient approach for constructing thermodynamically consistent constitutive models.
- Advantages of the proposed framework include the ease in developing increasingly complex constitutive models by mixing and matching re-usable components from a library of convex base functions in a systematic manner.
- This paper also describes the use of the modified LogSumExp (MLSE) function as a general and smooth approximation to the pointwise maximum function for any yield function (e.g. the Mohr-Coulomb/Tresca yield function). The MLSE function is then used to develop several new yield functions such as a convex and smooth approximation of the Matsuoka-Nakai yield function, a generalised polygonal yield function and a ‘Reuleaux triangle’-shaped yield function.

1 Introduction

In the last two decades, there has been an increasing interest in developing thermodynamically consistent (i.e. satisfying the laws of thermodynamics) constitutive models for a variety of geomaterials (e.g. Collins and Houlsby 1997; Collins and Kelly 2002; Sheng et al. 2004; Li 2007; Coussy et al. 2010; Collins et al. 2010; Tengattini et al. 2016; Lai et al. 2016; Zhang et al. 2018). There are generally two ways to ensure thermodynamic consistency in the constitutive model. One is to specify the model freely without constraints and then carry out retrospective checks to verify that the model specification satisfies the laws of thermodynamics; this process may be cumbersome, depending on the complexity of the model. The second is to specify the model with predefined constraints that automatically ensure thermodynamic consistency; this avoids the need for any retrospective checks, which makes for a more convenient process. One such approach is the 'hyperplasticity' constitutive modelling framework (Houlsby and Puzrin 2006).

Hyperplasticity is a framework for constructing thermodynamically consistent constitutive models, using the principles of thermodynamics as the starting point. This framework builds upon the work of Ziegler (1977) in a series of publications (e.g. Houlsby 1981; Collins and Houlsby 1997; Houlsby and Puzrin 2000), and the entire approach is summarised in Houlsby and Puzrin (2006). The hyperplasticity framework uses the concept of internal variables to model the history of loading; the most basic elastoplastic model uses a single internal variable (to represent plastic strain), while more complex models use multiple internal variables (e.g. hardening variables). The hyperplasticity approach has much in common with the 'standard material' methodology, developed independently and represented in the key publications (Moreau 1970; Suquet 1982; Germain et al. 1983). The two approaches are expressed in slightly different terminology but lead to closely aligned results.

A key feature of the hyperplasticity framework is that a constitutive model is completely defined through the specification of two scalar-valued functions – a free energy function and a dissipation function. This is also a feature of the 'standard material' approach. The laws of

thermodynamics are automatically satisfied by applying certain constraints to these functions (e.g. the dissipation function should be non-negative). Using the concepts of potentials and Legendre Transforms, these two functions can be used to determine the elastic behaviour, yield function, flow rule, and hardening rule of the constitutive model.

However, the concept of defining the constitutive behaviour of a material through a free energy function and a dissipation function may be foreign to those who are more familiar with the conventional plasticity approach of directly defining the (i) elasticity law; (ii) yield function; (iii) plastic potential, and (iv) hardening law. Moreover, it is non-trivial to define the dissipation function, which is usually more difficult to specify than a yield function as it is a latent function that is not based on directly observable experimental data.

It is important to address the above challenges, as thermodynamic consistency helps avoid physically unrealistic results, especially for modern constitutive models which are becoming increasingly complex. Therefore, this paper aims to address these challenges by proposing a new framework termed ‘Convex Modular Modelling’ (CMM), which provides a convenient approach to constructing constitutive models within the hyperplasticity framework. The CMM framework completely defines a constitutive model through the specification of two convex scalar-valued functions – a free energy function and a yield function. The CMM framework has much in common with the ‘standard material’ approach proposed by Germain et al. (1983), which suggests that all the constitutive equations of the material can be encapsulated in two non-negative convex closed functions. However, the main novelty of CMM is its modular nature, which makes it easier to construct custom convex functions for increasingly complex constitutive behaviour.

The main contributions of the paper are: (i) it describes the methodology and rules underlying the CMM framework, which provides a convenient approach for constructing thermodynamically consistent constitutive models within hyperplasticity theory; (ii) it demonstrates how the CMM framework can be used to build increasingly complex constitutive models by mixing and matching re-usable components from a library of convex base functions in a systematic manner.

For example, CMM is used to develop new convex yield functions such as a generalised polygonal yield function, an approximation of the Matsuoka-Nakai yield function and a convex capped yield function to restrict compressive strength; (iii) it describes the use of the modified LogSumExp function as a convex, smooth approximation to the pointwise maximum function. Unlike existing smooth approximations which are customised for specific yield functions such as the Mohr-Coulomb yield function, the modified LogSumExp function is a general and direct replacement for the pointwise max function in any yield function.

2 Hyperplasticity Theory

This section briefly describes the hyperplasticity framework, before introducing the CMM framework. Although the hyperplasticity framework is applicable to rate-independent or rate-dependent materials, the current paper focuses on rate-independent materials and isothermal conditions. Unless otherwise stated, the indicial notation is adopted here, where x, x_i, x_{ij}, x_{ijkl} correspond to a scalar, vector, matrix and rank-4 tensor respectively. The summation convention over the repeated index is implied (i.e. $a_i b_i = \sum_i a_i b_i$). However, this paper also uses the vector notation for the section on support functions, as the corresponding discussion is clearer in this notation.

2.1 Standard approach

The standard hyperplasticity approach (Housby and Puzrin 2006) completely defines a constitutive model through the specification of two scalar-valued functions – a free energy function and a dissipation function. The free energy function may be defined in terms of the Gibbs or Helmholtz free energy (with stress σ_{ij} or strain ε_{ij} as the independent variable, respectively). These free energy functions are not independent, but are related through a Legendre Transform. For this presentation, the Helmholtz free energy $f(\varepsilon_{ij}, \alpha_{ij})$ is adopted, where α_{ij} is an internal variable (which generally play the roles of 'generalised strains' such as

plastic strain). For simplicity, this presentation assumes only one internal variable, although multiple internal variables can be accommodated.

The dissipation function $d(\varepsilon_{ij}, \alpha_{ij}, \dot{\alpha}_{ij})$ must be non-negative and a homogeneous first order function of $\dot{\alpha}_{ij}$ for rate-independent materials i.e.

$$d = \frac{\partial d}{\partial \dot{\alpha}_{ij}} \dot{\alpha}_{ij}, \qquad d \geq 0 \tag{1}$$

The standard approach then defines $\sigma_{ij} = \frac{\partial f}{\partial \varepsilon_{ij}}, \chi_{ij} = \frac{\partial d}{\partial \dot{\alpha}_{ij}}$ and $\overline{\chi}_{ij} = -\frac{\partial f}{\partial \alpha_{ij}}$, where χ_{ij} and $\overline{\chi}_{ij}$ are 'generalised stresses' conjugate to $\dot{\alpha}_{ij}$ and α_{ij} respectively. It can be shown from thermodynamics (Houlsby and Puzrin 2006) that:

$$\left(\chi_{ij} - \overline{\chi}_{ij}\right) \dot{\alpha}_{ij} = 0 \tag{2}$$

The orthogonality postulate of Ziegler (1977) (i.e. $\chi_{ij} = \overline{\chi}_{ij}$) is then adopted and the entire constitutive response can now be derived without any further assumptions.

2.2 Convex approach

This section describes an alternative approach within the hyperplasticity framework, which allows for construction of constitutive models in a manner that is more similar to the conventional plasticity approach. This approach completely defines a constitutive model through the specification of two scalar-valued convex functions – a free energy function and a yield function. The existence of these functions can be shown using Legendre Transforms (Collins and Houlsby 1997; Houlsby and Puzrin 2006). The free energy function can be either the Helmholtz free energy function $f(\varepsilon_{ij}, \alpha_{ij})$ or the complementary free energy function $C(\sigma_{ij}, \alpha_{ij})$, which is the negative of the Gibbs free energy function. The complementary free energy function is adopted here instead of the Gibbs free energy function, as convexity is preserved when switching between the Helmholtz and complementary free energy function using Legendre Transforms. The yield function is denoted as $y(\sigma_{ij}, \alpha_{ij}, \chi_{ij})$.

$f(\varepsilon_{ij}, \alpha_{ij})$ (or $C(\sigma_{ij}, \alpha_{ij})$) must be convex in ε_{ij} (or σ_{ij}) to ensure non-negativity of the work done before yielding occurs and for the elastic stiffness matrix $\frac{\partial^2 f}{\partial \varepsilon_{ij} \partial \varepsilon_{kl}}$ (or elastic compliance matrix $\frac{\partial^2 \mathrm{C}}{\partial \sigma_{ij} \partial \sigma_{kl}}$) to be positive definite and thus, invertible. As for the yield function, $y(\sigma_{ij}, \alpha_{ij}, \chi_{ij})$ must be convex and enclose the origin in χ_{ij}. Note that a convex yield function should not be confused with a convex yield surface. Convexity of the yield surface does not necessarily imply convexity of the yield function, although the converse is true (see Appendix A).

In a similar way to conventional plasticity, the admissible stress space is $y \leq 0$ and the yield condition is $y = 0$. y also acts as the flow potential (Houlsby and Puzrin 2006) through:

$$\dot{\alpha}_{ij} = \lambda \frac{\partial y}{\partial \chi_{ij}} \tag{3}$$

where $\lambda \geq 0$ is a non-negative multiplier that is determined by the consistency condition $\dot{y} = 0$, and the Karush-Kuhn-Tucker (KKT) conditions apply: $\lambda y = 0$, $y \leq 0$ and $\lambda \geq 0$. Substituting Eq. 3 into Eq. 1 gives:

$$d = \lambda \frac{\partial \mathrm{y}}{\partial \chi_{ij}} \chi_{ij}, \qquad d \geq 0 \tag{4}$$

Since $\lambda \geq 0$, Eq. 4 is satisfied if:

$$\frac{\partial \mathrm{y}}{\partial \chi_{ij}} \chi_{ij} \geq 0 \tag{5}$$

which is true if the yield function is convex in χ_{ij} (see Appendix B).

The hyperplasticity approach allows either the dissipation or yield function to be specified, but this paper concentrates on the yield function because of advantages such as easier calibration against laboratory data. A side benefit of the convex approach is that the convexity of the yield function provides numerical robustness when applying implicit stress-update algorithms (Panteghini and Lagioia 2014). The convex approach is similar to the conventional plasticity approach, except that (i) a free energy function is defined for the elasticity law, instead of an elastic stiffness matrix (ii) the flow rule is with respect to χ_{ij}, instead of σ_{ij}, and the implications of this will become apparent later when associated and non-associated flow is addressed; (iii)

there is no separate plastic potential and yield function for non-associated flow. Instead, the yield function achieves this using two variables, σ_{ij} and χ_{ij}.

3 Convex Modular Modelling (CMM)

The CMM framework is a modular framework that eases the formulation of the convex scalar functions required for the convex approach within the hyperplasticity framework. The CMM framework is re-usable and extensible, which allows the development of constitutive models in a methodical manner. The key idea behind the CMM framework is that complex, convex functions can be constructed from a library of simple base functions that are *a priori* known to be convex. Each of these convex base functions are typically used to model a specific soil behaviour (e.g. mean pressure dependency of the yield function). A list of common convex base functions can be found in Table 1, although a more comprehensive list of well-known convex functions can be found in Boyd and Vandenberghe (2004). New convex functions for different yield surface shapes may also be developed using the flexible sum of squares convex (SOS-convex) polynomial approach described in Suryasentana et al. (2020, 2021). Note that linear and affine functions are both convex and concave.

The modular nature of the CMM framework then enables modelling of complex behaviour through the combination of these base functions. However, these combinations should be carried out using the following convexity-preserving rules (Boyd and Vandenberghe 2004):

Rule 1) Non-negative weighted sums

If $w_i \geq 0$ and f_i are convex functions, then $\sum_i w_i f_i$ is a convex function. This property extends to infinite sums and integrals.

Rule 2) Composition

If f is a convex function, $f(g_1, \dots, g_n)$ is convex if for each scalar-valued function g_i, one of the following conditions applies:

a) f is non-decreasing in each argument and g_i is convex.
b) f is non-increasing in each argument and g_i is concave.
c) g_i is affine or constant.

Rule 3) Pointwise maximum of convex functions

$\max(g_1, \ldots, g_n)$ is a convex function if each scalar-valued function g_i is convex.

Rule 4) Pointwise supremum of convex functions

If $g(x, a)$ is convex in x for each $a \in A$, then $\sup_{a \in A} g(x, a)$ is a convex in x over the set A.

Rule 5) Perspective of convex functions

The perspective of a function $g(x)$ is defined as $f(x, t) = tg(\frac{x}{t})$ for $t > 0$. If $g(x)$ is a convex function, $f(x, t)$ is a convex function too.

For convenience, the above convexity-preserving rules will be referred to as 'CMM Rule 1 to 5'.

4 Applications of CMM

This section demonstrates the application of the CMM framework in constructing constitutive models in a systematic and hierarchical manner. For clarity, this section will explore constitutive models from the familiar to the unfamiliar, and from simple to complex. Note that $\sigma_{ij}, \varepsilon_{ij}$ and χ_{ij} are assumed to be positive in compression. Any rank-2 tensor term with a prime superscript (e.g. χ'_{ij}, ε'_{ij}) is the deviatoric component. Unless otherwise stated, when it is stated that $f(\varepsilon_{ij}, \alpha_{ij})$ or $y(\sigma_{ij}, \alpha_{ij}, \chi_{ij})$ is convex, it is with respect to ε_{ij} and χ_{ij}, respectively. Note that due to CMM Rule 2c, if a function is convex in χ'_{ij} (or ε'_{ij}), it is also convex in χ_{ij} (or ε_{ij}). In this section, α_{ij} plays the role of the plastic strain. Table 1 contains the definitions of the basic building blocks of the CMM framework that are heavily used in this section, such as $J_2(\chi_{ij}), I_1(\chi_{ij}), p(\chi_{ij})$, which represent the 2nd deviatoric stress invariant function, 1st stress invariant function and mean stress function, respectively.

4.1 Free energy function

For isotropic linear elasticity (Houlsby and Puzrin 2006), the Helmholtz free energy function is:

$$f(\varepsilon_{ij}, \alpha_{ij}) = \frac{1}{2}K(\varepsilon_{ii} - \alpha_{ii})(\varepsilon_{jj} - \alpha_{jj}) + G\left(\varepsilon'_{ij} - \alpha'_{ij}\right)\left(\varepsilon'_{ij} - \alpha'_{ij}\right) \tag{6}$$

$$= \frac{1}{2}KI_1^2(\varepsilon_{ij} - \alpha_{ij}) + 2GJ_2(\varepsilon_{ij} - \alpha_{ij})$$

where K and G are the bulk modulus and shear modulus respectively. Eq. 6 is convex due to CMM Rule 1 (non-negative weighted sum of two convex functions as per Table 1, assuming $K \geq 0$ and $G \geq 0$) and Rule 2c ($\varepsilon_{ij} - \alpha_{ij}$ is an affine function of ε_{ij}).

For geomaterials, the elastic modulus typically varies as a power function of the mean stress. The free energy function proposed by Houlsby et al. (2005) may be used as its convexity has been confirmed by Lagioia and Panteghini (2019), who investigates the convexity of several existing hyperelastic free energy functions for soils. Lagioia and Panteghini (2019) also proposed a new convex hyperelastic free energy function (in both the Helmholtz and complementary forms), which approximates the hypoelastic constitutive relation adopted in models based on the Critical State framework (e.g. the Modified Cam-Clay) with a constant Poisson's ratio. To define the free energy functions for non-linear anisotropic elastic behaviour, readers may refer to Houlsby et al. (2019).

4.2 Classical yield functions

An additional advantage of the CMM framework is that it provides a sufficient (but not necessary) condition to prove the convexity of existing yield functions, by showing that they can be built up by combining simpler convex functions using the CMM rules.

For example, the Mohr-Coulomb/Tresca yield function is:

$$y(\sigma_i, \alpha_i, \chi_i) = \max\begin{pmatrix} \pm\dfrac{(\chi_1 - \chi_2)}{2} - \dfrac{(\chi_1 + \chi_2)}{2}\sin\phi - c\cos\phi, \\ \pm\dfrac{(\chi_2 - \chi_3)}{2} - \dfrac{(\chi_2 + \chi_3)}{2}\sin\phi - c\cos\phi, \\ \pm\dfrac{(\chi_3 - \chi_1)}{2} - \dfrac{(\chi_3 + \chi_1)}{2}\sin\phi - c\cos\phi \end{pmatrix} \tag{7}$$

Eq. 7 is convex as it is the pointwise maximum of affine functions (CMM Rule 3).

Another example is the Drucker-Prager/Von Mises yield function:

$$y(\sigma_{ij}, \alpha_{ij}, \chi_{ij}) = \sqrt{J_2(\chi_{ij})} - mI_1(\chi_{ij}) - c \tag{8}$$

$\sqrt{J_2(\chi_{ij})}$ is a convex function (see Table 1) and $-mI_1(\chi_{ij}) - c$ is an affine function. Therefore, Eq. 8 is convex due to CMM Rule 1. To model non-associative flow in the true stress space σ_{ij}, the non-associative Drucker-Prager/Von Mises yield function may be defined as:

$$y(\sigma_{ij}, \alpha_{ij}, \chi_{ij}) = y_{\text{assoc}}(\sigma_{ij}, \alpha_{ij}, \chi_{ij}) + m_2 I_1(\sigma_{ij}) \tag{9}$$

where $y_{\text{assoc}}(\sigma_{ij}, \alpha_{ij}, \chi_{ij})$ refers to Eq. 8 and m_2 is the non-associative flow rule parameter. Eq. 9 is convex due to CMM Rule 1.

The final example is the 'Critical State'-based Modified Cam-Clay model, which forms the basis for many advanced constitutive models for geomaterials. Its yield function may be written as:

$$y(\sigma_{ij}, \alpha_{ij}, \chi_{ij}) = \chi_q^2 + M^2 \chi_p \left(\chi_p - p_c(\alpha_{ij})\right) \tag{10}$$

where χ_p and χ_p are the mean and deviatoric stresses in generalised triaxial stress space, and p_c and M are model parameters representing the pre-consolidation pressure and the slope of the critical state line, respectively. Eq. 10 may be rewritten as:

$$y(\sigma_{ij}, \alpha_{ij}, \chi_{ij}) = 3J_2(\chi_{ij}) + \frac{1}{9} M^2 I_1^2(\chi_{ij}) - M^2 p_c(\alpha_{ij}) p(\chi_{ij}) \tag{11}$$

where the convex functions $J_2(\chi_{ij}), I_1^2(\chi_{ij})$ and $p(\chi_{ij})$ are defined in Table 1. Note that σ_{ij} and χ_{ij} in Eq. 11 correspond to the effective stress components (i.e. total stress less pore pressure). Eq. 11 is convex due to CMM Rule 1, as it is the non-negative weighted sum of three convex functions, noting that the last term $-M^2 p_c(\alpha_{ij}) p(\chi_{ij})$ is a linear function in χ_{ij}.

4.3 Lode angle effect in yield functions

It is sometimes convenient to define yield functions in terms of the following set of stress invariants $\left\{I_1(\chi_{ij}), \sqrt{J_2(\chi_{ij})}, \theta(\chi_{ij})\right\}$, where θ is the Lode angle. It can be challenging to use this set of stress invariants within the hyperplasticity framework due to the difficulty in specifying the

effect of the Lode angle on the dissipation. The following will demonstrate how the Lode angle effects can be modelled within the CMM framework, thereby allowing specification of hyperplasticity-based constitutive models based on this set of stress invariants.

To allow the specification of a yield surface that varies with the Lode angle on the deviatoric plane, the following deviatoric shape function is defined:

$$J_\theta(\chi_{ij}) = \sqrt{J_2(\chi_{ij})} f_{\text{shape}}(\theta(\chi_{ij})) \tag{12}$$

where $f_{\text{shape}}(\theta(\chi_{ij}))$ controls the shape of the yield surface on the deviatoric plane. Although $\sqrt{J_2(\chi_{ij})}$ is a convex function, $J_\theta(\chi_{ij})$ is only convex if it satisfies some condition. Previous researchers (e.g. Abbo et al. 2011, Soare and Benzerga 2016) have identified the convexity condition for $J_\theta(\chi_{ij})$ as:

$$\frac{\partial^2 f_{\text{shape}}(\theta)}{\partial \theta^2} + f_{\text{shape}}(\theta) \geq 0, \qquad 0 \leq \theta \leq \frac{\pi}{3} \tag{13}$$

Interested readers may refer to Soare and Benzerga (2016) for a detailed derivation of Eq. 13. Recently, Lagioia and Panteghini (2016) proposed a new yield function that unifies several classical yield functions such as Drucker-Prager/von Mises, Mohr-Coulomb/Tresca, Matsuoka-Nakai and Lade-Duncan. The unified yield function, referred to as the Generalised Classical (GC) yield function by Lester and Sloan (2018), is of the following form:

$$y(\sigma_{ij}, \alpha_{ij}, \chi_{ij}) = J_\theta(\chi_{ij}) - mI_1(\chi_{ij}) - k \tag{14}$$

where m and k are material properties. If $J_\theta(\chi_{ij})$ is convex, Eq. 14 is convex too, due to CMM Rule 1. The shape function $f_{\text{shape}}(\theta)$ in $J_\theta(\chi_{ij})$ is defined as:

$$f_{\text{shape}}(\theta) = s_1 \cos\left(\frac{1}{3}\cos^{-1}(s_2 \sin 3\theta) - \frac{\pi}{6} s_3\right) \tag{15}$$

where s_1, s_2, s_3 are shape parameters whose values depend on the selected classical yield criterion (see Lagioia and Panteghini 2016, Lester and Sloan 2018).

Lester and Sloan (2018) conducted a numerical study to assess if Eq. 15 satisfies Eq. 13 and they found that Eq. 13 is satisfied for all of the classical yield criteria, except for the Outer Mohr-Coulomb criterion. This suggests that heuristically, $J_\theta(\chi_{ij})$ in conjuction with Eq. 15 is convex

and thus, may be used to model the Lode angle effect within the CMM framework for practical purposes.

5 Custom yield functions

This section now departs from the familiar constitutive models and demonstrates how the CMM framework can be utilised to develop new, custom convex yield functions.

5.1 Smooth approximation of non-smooth yield functions

The existence of gradient discontinuities in non-smooth yield functions (such as the Mohr-Coulomb/Tresca yield function) poses computational difficulties in stress update schemes, and there has been much research in removing these discontinuities to increase numerical robustness. For example, there are various techniques for eliminating the discontinuities in the Mohr-Coulomb yield function (e.g. Sloan and Booker 1986, Abbo and Sloan 1995, Abbo et al. 2011). However, most of these techniques are bespoke to specific yield functions and are not easily transferable to other non-smooth yield functions. The following describes the use of a modified LogSumExp (MLSE) function as a general technique to obtain a smooth, convex approximation of any non-smooth yield function which can be cast as a pointwise maximum of several convex functions.

The LogSumExp (LSE) function is the natural logarithm of the sum of exponentials of the arguments:

$$\mathrm{LSE}(x_1, \dots, x_n) = \log\left(\sum_{i=1}^{n} \exp(x_i)\right) \tag{16}$$

It is a convex function and is a smooth, differentiable and analytic approximation of the pointwise maximum function (Boyd and Vandenberghe 2004). Its gradient is defined as:

$$\frac{\partial \mathrm{LSE}}{\partial \mathrm{x}_j} = \frac{\exp(x_j)}{\sum_{i=1}^{n} \exp(x_i)}, \qquad j = 1 \dots n \tag{17}$$

Eq. 17 is usually called the 'softmax' function and ranges from 0 to 1. A key advantage of the LSE function is that it is at least C2 continuous (i.e. second-derivative is continuous), which allows for convenient numerical implementation in finite element programs (Abbo et al. 2011). A more general modified LogSumExp (MLSE) function is used here, which allows for control of how close the smooth approximation is to the original pointwise maximum function:

$$\mathrm{MLSE}(b, f_1, \dots, f_m) = \frac{1}{b}\mathrm{LSE}(bf_1, \dots, bf_m) \tag{18}$$

where $b > 0$ is a smoothening parameter and f_i is a convex function of the arguments $x_1, \dots, x_n$. The larger b is, the closer the MLSE smooth approximation is to the pointwise maximum function. Note that each bf_i should be dimensionless. Thus, the dimensions of b should be the inverse of the dimensions of f_i. Since LSE is a non-decreasing, convex function (Calafiore and Ghaoui 2014) and f_i is a convex function, MLSE is a convex function due to CMM Rule 2a. Its gradient is defined as:

$$\frac{\partial \mathrm{MLSE}}{\partial \mathrm{x}_j} = \frac{1}{b}\sum_{i=1}^{m} \frac{\partial \mathrm{LSE}}{\partial bf_i}\frac{\partial bf_i}{\partial f_i}\frac{\partial f_i}{\partial \mathrm{x}_j}, \qquad j = 1 \dots n \tag{19}$$

$$= \sum_{i=1}^{m}\left(\frac{\exp(bf_i)}{\sum_{k=1}^{n}\exp(bf_k)}\right)\frac{\partial f_i}{\partial \mathrm{x}_j}$$

The MLSE function can be used as a direct replacement for the pointwise maximum function. For example, the MLSE approximation of Mohr Coulomb/Tresca yield function (Eq. 7) is:

$$\mathrm{MLSE}\begin{pmatrix} b, \\ \frac{(\chi_1-\chi_2)}{2} - \frac{(\chi_1+\chi_2)}{2}\sin\phi - c\cos\phi, \\ \frac{(\chi_2-\chi_3)}{2} - \frac{(\chi_2+\chi_3)}{2}\sin\phi - c\cos\phi, \\ \frac{(\chi_3-\chi_1)}{2} - \frac{(\chi_3+\chi_1)}{2}\sin\phi - c\cos\phi \\ -\frac{(\chi_1-\chi_2)}{2} - \frac{(\chi_1+\chi_2)}{2}\sin\phi - c\cos\phi, \\ -\frac{(\chi_2-\chi_3)}{2} - \frac{(\chi_2+\chi_3)}{2}\sin\phi - c\cos\phi, \\ -\frac{(\chi_3-\chi_1)}{2} - \frac{(\chi_3+\chi_1)}{2}\sin\phi - c\cos\phi \end{pmatrix} \tag{20}$$

Eq. 20 is a convex function as each argument is an affine function or a constant (CMM Rule 2c). Figure 1 shows the MLSE approximation of the Tresca and Mohr Coulomb yield functions for 3 different b values ($b = 10/\sigma_r, 20/\sigma_r, 100/\sigma_r$ where σ_r is some reference yield strength value

such as the cohesive strength c). As can be observed, the MLSE approximation for $b = 100/\sigma_r$ is virtually identical to the original non-smooth criterion.

5.2 Generalised polygonal yield function

In convex analysis, a support function S_A of a set $A \subseteq R^n$ is defined as:

$$S_A(\boldsymbol{x}) = \sup_{\boldsymbol{a} \in A} \boldsymbol{x}^T \boldsymbol{a} \tag{21}$$

$S_A(\boldsymbol{x})$ is the pointwise supremum of affine functions and is hence convex (CMM Rule 4). The Mohr-Coulomb/Tresca yield function may be recast using a support function:

$$y(\sigma_i, \alpha_i, \chi_i) = S_A(\boldsymbol{x}) - c\cos\phi \tag{22}$$

where

$$\boldsymbol{x} = \begin{bmatrix} \chi_1 \\ \chi_2 \\ \chi_3 \end{bmatrix}, \qquad A = \{\boldsymbol{a_1}, \dots, \boldsymbol{a_6}\},$$

$$\boldsymbol{a_1} = \begin{bmatrix} \frac{1}{2} - \frac{1}{2}\sin\phi \\ -\frac{1}{2} - \frac{1}{2}\sin\phi \\ 0 \end{bmatrix}, \boldsymbol{a_2} = \begin{bmatrix} 0 \\ \frac{1}{2} - \frac{1}{2}\sin\phi \\ -\frac{1}{2} - \frac{1}{2}\sin\phi \end{bmatrix}, \boldsymbol{a_3} = \begin{bmatrix} -\frac{1}{2} - \frac{1}{2}\sin\phi \\ 0 \\ \frac{1}{2} - \frac{1}{2}\sin\phi \end{bmatrix},$$

$$\boldsymbol{a_4} = \begin{bmatrix} -\frac{1}{2} - \frac{1}{2}\sin\phi \\ \frac{1}{2} - \frac{1}{2}\sin\phi \\ 0 \end{bmatrix}, \boldsymbol{a_5} = \begin{bmatrix} 0 \\ -\frac{1}{2} - \frac{1}{2}\sin\phi \\ \frac{1}{2} - \frac{1}{2}\sin\phi \end{bmatrix}, \boldsymbol{a_6} = \begin{bmatrix} \frac{1}{2} - \frac{1}{2}\sin\phi \\ 0 \\ -\frac{1}{2} - \frac{1}{2}\sin\phi \end{bmatrix}$$

$\boldsymbol{a_1}, \dots, \boldsymbol{a_6}$ are the normal vectors of the hyperplanes that collectively represent the piecewise linear yield surface. If $\boldsymbol{a_1}, \dots, \boldsymbol{a_6}$ are unit vectors, the normal distance between each hyperplane and the origin of the stress space is $c\cos\phi$. Eq. 22 is convex due to CMM Rule 1, noting that $-c\cos\phi$ is a constant.

A convex polyhedron yield function can therefore be used to define a piecewise linear approximation of any arbitrary-shaped yield surface, simply by defining the normal vectors of the hyperplanes that represent the piecewise-linear sides of the polyhedron. The following shows how to define a pressure-independent, generalised polygonal yield function using this concept.

Let $e_y = \frac{1}{\sqrt{6}}\begin{bmatrix} 2 \\ -1 \\ -1 \end{bmatrix}$ be the unit vector that is parallel to the projection of the χ_1 axis on the deviatoric plane and $e_x = \frac{1}{\sqrt{2}}\begin{bmatrix} 0 \\ -1 \\ 1 \end{bmatrix}$ be the unit vector that is orthogonal to e_y and lies on the deviatoric plane, as shown in Fig. 2. A generalised vector e_θ that points in any arbitrary direction along the deviatoric plane can be defined in terms of e_y and e_x, where θ is the Lode angle:

$$e_\theta = e_y \cos\theta - e_x \sin\theta \tag{23}$$

Using Eq. 23, a 3-sided polygonal yield function can be defined as:

$$y(\sigma_i, \alpha_i, \chi_i) = S_A(\boldsymbol{x}) - c \tag{24}$$

where

$$\boldsymbol{x} = \begin{bmatrix} \chi_1 \\ \chi_2 \\ \chi_3 \end{bmatrix}, \qquad A = \{\boldsymbol{a_1}, \boldsymbol{a_2}, \boldsymbol{a_3}\},$$

$$\boldsymbol{a_1} = \begin{bmatrix} 0.4082 \\ 0.4082 \\ -0.8165 \end{bmatrix}, \boldsymbol{a_2} = \begin{bmatrix} 0.4082 \\ -0.8165 \\ 0.4082 \end{bmatrix}, \boldsymbol{a_3} = \begin{bmatrix} -0.8165 \\ 0.4082 \\ 0.4082 \end{bmatrix},$$

Here, $\boldsymbol{a_1}, \dots, \boldsymbol{a_3}$ are obtained by substituting $\theta = \frac{\pi}{3}, -\frac{\pi}{3}, \pi$ into Eq. 23**,** and they represent the unit normal vectors of the three hyperplanes that collectively represent the piecewise linear yield surface. As these are unit vectors, the projected normal distances of all the hyperplanes from origin of the stress space are c, as shown in Fig. 3.

Similarly, a 12-sided polygonal yield function can be obtained by substituting into Eq. 23 the Lode angles for each normal vector of the 12 hyperplanes representing the polygon sides. Fig. 4 illustrates the 12-sided polygonal yield surface in the deviatoric plane. Therefore, with a sufficient number of hyperplanes, one could potentially model a reasonably close approximation of an arbitrarily shaped yield surface. For computational implementation, the MLSE function may be used to approximate these 'support function'-based yield functions. For example, Eq. 24 can be approximated as:

$$y(\sigma_i, \alpha_i, \chi_i) = \mathrm{MLSE}\begin{pmatrix} b, \\ 0.4082\chi_1 + 0.4082\chi_2 - 0.8165\chi_3 - c, \\ 0.4082\chi_1 - 0.8165\chi_2 + 0.4082\chi_3 - c, \\ -0.8165\chi_1 + 0.4082\chi_2 + 0.4082\chi_3 - c \end{pmatrix} \tag{25}$$

5.3 Convex approximating yield functions

The Matsuoka-Nakai yield criterion is widely used for modelling cohesionless soil, as its yield surface is a good fit with experimental data, especially in the deviatoric plane. However, it is not convex throughout its domain in its original form (Panteghini and Lagioia 2014). A convex approximation of the Matsuoka-Nakai yield function is developed here by combining the Mohr-Coulomb yield function and the MLSE function as follows:

$$y(\sigma_i, \alpha_i, \chi_i) = \text{MLSE}\begin{pmatrix} b(\phi), \\ \frac{(\chi_1-\chi_2)}{2} - \frac{(\chi_1+\chi_2)}{2}\sin\phi - c_1\cos\phi\,, \\ \frac{(\chi_2-\chi_3)}{2} - \frac{(\chi_2+\chi_3)}{2}\sin\phi - c_1\cos\phi\,, \\ \frac{(\chi_3-\chi_1)}{2} - \frac{(\chi_3+\chi_1)}{2}\sin\phi - c_1\cos\phi \\ -\frac{(\chi_1-\chi_2)}{2} - \frac{(\chi_1+\chi_2)}{2}\sin\phi - c_1\cos\phi\,, \\ -\frac{(\chi_2-\chi_3)}{2} - \frac{(\chi_2+\chi_3)}{2}\sin\phi - c_1\cos\phi\,, \\ -\frac{(\chi_3-\chi_1)}{2} - \frac{(\chi_3+\chi_1)}{2}\sin\phi - c_1\cos\phi \end{pmatrix} \tag{26}$$

where

$$b(\phi) = \frac{5}{\left(1.001-\left(\frac{\phi}{\pi/2}\right)^{1.5}\right)c_1} \quad \text{for } 0 \le \phi \le \frac{\pi}{2} \tag{27}$$

The main differences between Eq. 26 and Eq. 20 are that b is now a function of ϕ and its representative cohesive strength is $c_1 = 1.14c$, where c is the true cohesive strength of the material. Thus, the expressions in Eq. 26 define a 'bounding support function' in the form of a slightly enlarged Mohr Coulomb yield function, and the convex approximation of the Matsuoka-Nakai yield function is inscribed within it, where $b(\phi)$ controls how close the approximating yield function is to the bounding support function. Fig. 5 compares the approximating yield function with the original Matsuoka-Nakai yield function in the deviatoric plane, where it is evident that they agree very well. While the GC-based Matsuoka-Nakai yield function (Eq. 13) has a numerical-based convexity check, Eq. 26 has an analytical convexity proof (see previous discussion on the convexity for Eq. 20).

To demonstrate further how a more complex convex yield function can be built up by combining simpler convex functions, a convex and smooth 'Reuleaux triangle'-shaped pressure-independent yield function is developed here, which is similar to the 'modified Reuleaux triangle' yield functions defined in the literature (e.g. Coombs et al. 2010; Coombs and Crouch 2011). This custom yield function is a convex combination of a circular yield function, which is modelled using the Von Mises yield function (Eq. 8), and a triangular yield function, which is modelled using the 3-sided polygon yield function (Eq. 24). Therefore, the convex 'Reuleaux triangle'-shaped yield function is defined as:

$$y(\sigma_i, \alpha_i, \chi_i) = (1-w)\left(\sqrt{J_2(\chi_i)} - c\right) + (w)MLSE\left(\frac{100}{c}, \boldsymbol{x}^T\boldsymbol{a_1} - \frac{c}{\sqrt{2}}, \boldsymbol{x}^T\boldsymbol{a_2} - \frac{c}{\sqrt{2}}, \boldsymbol{x}^T\boldsymbol{a_3} - \frac{c}{\sqrt{2}}\right) \tag{28}$$

where

$$\boldsymbol{x} = \begin{bmatrix}\chi_1\\ \chi_2\\ \chi_3\end{bmatrix}, \quad \boldsymbol{a_1} = \begin{bmatrix}0.4082\\ 0.4082\\ -0.8165\end{bmatrix}, \boldsymbol{a_2} = \begin{bmatrix}0.4082\\ -0.8165\\ 0.4082\end{bmatrix}, \boldsymbol{a_3} = \begin{bmatrix}-0.8165\\ 0.4082\\ 0.4082\end{bmatrix}$$

Here, $0 \leq w \leq 1$ controls the curvature of the Reuleaux triangle yield surface in the deviatoric plane, as shown in Fig. 6. Since the expression $\sqrt{J_2(\chi_i)} - c$ and the $MLSE$ function are both convex, Eq. 28 is convex due to CMM Rule 1.

5.4 Capped yield functions

Capped yield functions can be implemented in the CMM framework using the following 'template':

$$y_{\text{capped}}(\sigma_{ij}, \alpha_{ij}, \chi_{ij}) = MLSE\left(b, y_{\text{uncapped}}(\sigma_{ij}, \alpha_{ij}, \chi_{ij}), y_{\text{cap\_1}}(\sigma_{ij}, \alpha_{ij}, \chi_{ij}), \dots, y_{\text{cap\_n}}(\sigma_{ij}, \alpha_{ij}, \chi_{ij})\right) \tag{29}$$

Eq. 29 defines a capped yield function y_{capped} by using the MLSE function to combine the original uncapped yield function y_{uncapped} with an arbitrary number of 'cap' yield functions $y_{\text{cap\_i}}$. The main constraint that needs to be obeyed is that each yield function in Eq. 29 (i.e. $y_{\text{uncapped}}, y_{\text{cap\_1}}, \dots, y_{\text{cap\_n}}$) must be convex, in order to ensure that y_{capped} is convex.

To demonstrate this, a convex capped version of the Drucker-Prager yield function (Eq. 8) is developed here by combining it with an elliptical cap $y_{\text{cap\_c}}$ to limit compressive strength.

$$y_{\text{capped}}(\sigma_{ij}, \alpha_{ij}, \chi_{ij}) = MLSE\left(b, y_{\text{uncapped}}(\sigma_{ij}, \alpha_{ij}, \chi_{ij}), y_{\text{cap\_c}}(\sigma_{ij}, \alpha_{ij}, \chi_{ij})\right) \tag{30}$$

where

$$y_{\text{cap\_c}}(\sigma_{ij}, \alpha_{ij}, \chi_{ij}) = \frac{J_2(\chi_{ij})}{M_q^2} + \frac{\left(I_1(\chi_{ij}) - p_0\right)^2}{M_p^2} - 1 \tag{31}$$

Here, $b = 100/c$, y_{uncapped} is the Drucker-Prager yield function and p_0, M_q and M_p are material properties. $y_{\text{cap\_c}}$ can be shown to be convex functions using CMM Rule 1. Fig. 7 shows an example of the yield surface of Eq. 30 in the meridional plane, which shows that the MLSE function allows for a straightforward generation of convex capped constitutive models, bounded by (potentially) an arbitrary number of caps of varying shapes.

6 Discussion

This paper sets out a framework for convenient construction of thermodynamically consistent constitutive models. The simplicity of the proposed CMM framework has been demonstrated by developing a wide range of constitutive models through a systematic combination of convex base functions. Constructing models within the CMM framework is similar to that of the conventional plasticity approach, except that special care must be taken to ensure convexity of the free energy and yield functions.

Besides developing new constitutive models, the CMM framework also provides a sufficient (but not necessary) condition for proving the convexity (and thus thermodynamic consistency) of existing models (such as the classical Drucker Prager/Von Mises, Mohr Coulomb/Tresca and Modified Cam-Clay models shown in this paper). Note that there exist constitutive models that are thermodynamically consistent, but cannot be proven using the CMM rules, such as models that uses SOS-convex polynomial based yield functions (Suryasentana et al. 2020, 2021).

One of the benefits of smooth, convex yield functions is that they provide numerical robustness during the elastoplastic stress updates. For example, Fig. 8 shows an element with the smooth MLSE-based Tresca yield function (Eq. 20) undergoing a strain-controlled stress path from the origin of the stress path to the yield surface, and then travelling along the yield surface. Three smoothening values $b = 10/c, 20/c, 100/c$ were implemented, and the computational time is similar for all b values and no numerical difficulties were encountered at the vertices. The key constitutive equations for the numerical implementation can be found in Appendix C. It should be noted that smoothness in yield functions is not necessary for numerical efficiency, as there exists specialised algorithms (e.g. de Souza Neto et al. 2008) for efficient handling of non-smoothness on the yield surface, as has been used successfully by previous researchers (e.g. Panteghini and Lagioia 2014, 2018, 2019). Nevertheless, one of the key advantages of smooth, convex yield functions is that they can be handled by the standard algorithms typically used in most finite element codes.

It has been noted in the literature (e.g. Panteghini and Lagioia 2018) that yield and plastic potential surfaces are often affected by problems related to convexity. One such problem is the case where the yield surface that bounds the elastic domain (i.e. $f \leq 0$) is convex, but the surfaces outside the elastic domain (i.e. $f > 0$) are not convex. This creates problems in the numerical integration of the constitutive law, especially when using implicit integration schemes. This problem is avoided with the CMM framework, as the framework guarantees that all yield surfaces are convex, including those corresponding to $f > 0$. This comes from convex analysis theory that states that if a function f is convex, its k-sublevel sets $\{x|f(x) \leq k\}$ are necessarily convex for any value of k (Boyd and Vandenberghe 2004). This means that not only is the actual yield surface (which is a 0-level sublevel set $\{x|f(x) \leq 0\}$) convex, the 'inadmissible' yield surfaces corresponding to $f > 0$ are also convex. To illustrate this, Fig. 9 shows the contour plots of the yield surfaces for the approximate Matsuoka-Nakai yield function (Eq. 26) and the capped yield function (Eq. 30) for $f = 0, 0.5, 1, 2$. It is evident that all the surfaces are convex, including those corresponding to $f > 0$.

Although the applications shown in this paper do not capture complex material behaviour such as anisotropy, it should be emphasised that the main purpose of this paper is not to describe a sophisticated model, but to introduce the components of the framework for constructing new constitutive models in a methodical and hierarchical manner. Nevertheless, more complex constitutive models can be constructed within this framework. For example, to capture realistic behaviour of geomaterials under cyclic loading (e.g. hysteresis, Bauschinger effect, ratcheting), a multi-surface kinematic hardening with ratcheting extension of any convex yield function can be developed, following Houlsby et al. (2017):

$$y^{(n)}\left(\sigma_{ij}, \alpha_{ij}^{(n)}, \chi_{ij}^{(n)}, \alpha_{ij}^{r}, \chi_{ij}^{r}\right) = y_{\text{convex}}\left(\sigma_{ij}, \alpha_{ij}^{(n)}, \chi_{ij}^{(n)}\right) + R_n\left(\sqrt{J_2\left(\chi_{ij}^{r}\right)} - \sqrt{J_2\left(\sigma_{ij}\right)}\right) \tag{32}$$

where y_{convex} is any valid convex yield function (e.g. Von Mises), N is the number of yield surfaces and the $^{(n)}$ superscript refers to the entity corresponding to the nth surface. χ_{ij}^{r} is the generalised stress conjugate to the ratcheting strain α_{ij}^{r} and $R_n \geq 0$ is a modelling parameter. It can be shown that Eq. 32 is convex due to CMM Rule 1.

It is envisaged that as more convex base functions are derived and added to Table 1, the modelling flexibility of the framework will greatly expand. The simplicity of the CMM framework is highlighted: this is merely the starting point for more realistic (and advanced) thermodynamically consistent constitutive models.

7 Conclusions

The CMM is a flexible framework capable of building highly modular, thermodynamically consistent constitutive models. It proposes a new convex approach to developing constitutive models within the hyperplasticity framework, which does not require any knowledge or specification of the dissipation function (a task that is not always straightforward). This paper has shown several examples on how to develop increasingly complex constitutive models through combination of modular convex base functions according to the CMM rules. It is simple to use and potentially offers a more accessible path for constitutive modellers to take advantage of the hyperplasticity framework to develop robust constitutive models.

8 Acknowledgements

Parts of the work described here were conducted when the first author was at the University of Oxford. The first author would like to thank Professor Byron Byrne and Professor Harvey Burd for their generous support during his time there.

9 Appendix

A: Convex Functions

A function f is defined to be convex if its domain is a convex set and,

$$f(w\boldsymbol{x} + (1-w)\boldsymbol{y}) \leq wf(\boldsymbol{x}) + (1-w)f(\boldsymbol{y}) \quad \text{A1}$$

for all $\boldsymbol{x}, \boldsymbol{y} \in$ domain of f and for $0 \leq w \leq 1$ (Boyd and Vandenberghe 2004). Depending on the differentiability of f, there are two equivalent conditions to Eq. A1.

If f is differentiable, f is convex if its domain is a convex set (Boyd and Vandenberghe 2004) and

$$f(\boldsymbol{y}) \geq f(\boldsymbol{x}) + \nabla f(\boldsymbol{x})^{\mathrm{T}}(\boldsymbol{y} - \boldsymbol{x}) \quad \text{A2}$$

for all $\boldsymbol{x}, \boldsymbol{y} \in$ domain of f. This is known as the 'first-order condition'.

If f is twice differentiable, f is convex if its domain is a convex set and $\nabla^2 f(\boldsymbol{x})$ is positive semidefinite everywhere in its domain i.e.

$$\boldsymbol{y}^{\mathrm{T}} \nabla^2 f(\boldsymbol{x}) \boldsymbol{y} \geq 0 \quad \text{A3}$$

for all $\boldsymbol{x}, \boldsymbol{y} \in$ domain of f. This is known as the 'second-order condition'.

A yield surface is not identical to a yield function. A yield surface is usually defined as the zero level set of a yield function $f(x)$ (i.e. $\{x | f(x) = 0\}$). A convex yield surface does not necessarily imply convexity of $f(x)$. However, if $f(x)$ is convex, then the yield surface is necessarily convex. This is due to convex analysis relating convex functions and their sub-level sets (Boyd and Vandenberghe 2004), where a *k*-sublevel set is defined as $\{x | f(x) \leq k\}$.

B: Fulfilment of Eq. 5 through convexity of the yield function

Following the notation of Ottosen and Ristinmaa (2005), it is convenient to define the sets $\boldsymbol{\chi} = \left\{\chi_{ij}^{(1)}, \dots, \chi_{ij}^{(n)}\right\}$ and $\boldsymbol{\alpha} = \left\{\alpha_{ij}^{(1)}, \dots, \alpha_{ij}^{(n)}\right\}$, where $\alpha_{ij}^{(1)}, \dots, \alpha_{ij}^{(n)}$ are n number of internal variables and $\chi_{ij}^{(1)}, \dots, \chi_{ij}^{(n)}$ are their corresponding generalised stresses.

Since y is defined to be convex in $\boldsymbol{\chi}$, the first-order condition of convex functions gives:

$$y(\sigma_{ij}, \boldsymbol{\alpha}, \boldsymbol{\chi}_1) \geq y(\sigma_{ij}, \boldsymbol{\alpha}, \boldsymbol{\chi}_0) + \frac{\partial \mathrm{y}}{\partial \boldsymbol{\chi}}\Big|_{\boldsymbol{\chi}_0} (\boldsymbol{\chi}_1 - \boldsymbol{\chi}_0) \tag{B1}$$

$$\frac{\partial \mathrm{y}}{\partial \boldsymbol{\chi}}\Big|_{\boldsymbol{\chi}_0} (\boldsymbol{\chi}_0 - \boldsymbol{\chi}_1) \geq y(\sigma_{ij}, \boldsymbol{\alpha}, \boldsymbol{\chi}_0) - y(\sigma_{ij}, \boldsymbol{\alpha}, \boldsymbol{\chi}_1)$$

Let $\boldsymbol{\chi}_1 = \{\boldsymbol{\chi} | y(\sigma_{ij}, \boldsymbol{\alpha}, \boldsymbol{\chi}) \leq 0\}$ (i.e. the set of $\boldsymbol{\chi}$ that lies inside or on the yield surface) and $\boldsymbol{\chi}_0 = \{\boldsymbol{\chi} | y(\sigma_{ij}, \boldsymbol{\alpha}, \boldsymbol{\chi}) = 0\}$ (i.e. the set of $\boldsymbol{\chi}$ that lies on the yield surface). Since $y(\sigma_{ij}, \boldsymbol{\alpha}, \boldsymbol{\chi}_0) = 0$ and $y(\sigma_{ij}, \boldsymbol{\alpha}, \boldsymbol{\chi}_1) \leq 0$, it follows that:

$$\frac{\partial \mathrm{y}}{\partial \boldsymbol{\chi}}\Big|_{\boldsymbol{\chi}_0} (\boldsymbol{\chi}_0 - \boldsymbol{\chi}_1) \geq 0 \tag{B2}$$

Substituting $\boldsymbol{\chi}_1 = \mathbf{0} = \{0, \dots, 0\}$ then gives:

$$\frac{\partial \mathrm{y}}{\partial \boldsymbol{\chi}}\Big|_{\boldsymbol{\chi}_0} (\boldsymbol{\chi}_0) \geq 0 \tag{B3}$$

Let $\boldsymbol{\chi}$ be $\boldsymbol{\chi}_0$:

$$\frac{\partial \mathrm{y}}{\partial \boldsymbol{\chi}} \boldsymbol{\chi} \geq 0 \tag{B4}$$

Hence, Eq. 5 is satisfied.

C: Key constitutive equations for numerical implementation of Figure 8

The free energy function is defined to be Eq. 6 and the yield function is defined to be Eq. 20 (for $\phi = 0$). These two convex functions are all that is required to determine the key constitutive equations based on the hyperplasticity framework, as follows:

$$\sigma_{ij} = \frac{\partial f}{\partial \varepsilon_{ij}} \tag{C1}$$

$$= K(\varepsilon_{kk} - \alpha_{kk})\delta_{ij} + 2G\left(\varepsilon'_{ij} - \alpha'_{ij}\right)$$

$$\bar{\chi}_{ij} = -\frac{\partial f}{\partial \alpha_{ij}} \tag{C2}$$

$$= K(\varepsilon_{kk} - \alpha_{kk})\delta_{ij} + 2G\left(\varepsilon'_{ij} - \alpha'_{ij}\right)$$

$$\frac{\partial \sigma_{ij}}{\partial \varepsilon_{kl}} = \frac{\partial^2 f}{\partial \varepsilon_{ij}\varepsilon_{kl}} \tag{C3}$$

$$= \left(K - \frac{2G}{3}\right)\delta_{ij}\delta_{kl} + 2G\delta_{ik}\delta_{jl}$$

$$\frac{\partial \sigma_{ij}}{\partial \alpha_{kl}} = \frac{\partial^2 f}{\partial \varepsilon_{ij}\alpha_{kl}} \tag{C4}$$

$$= -\left(K - \frac{2G}{3}\right)\delta_{ij}\delta_{kl} - 2G\delta_{ik}\delta_{jl}$$

$$-\frac{\partial \bar{\chi}_{ij}}{\partial \varepsilon_{kl}} = \frac{\partial^2 f}{\partial \alpha_{ij}\varepsilon_{kl}} \tag{C5}$$

$$= -\left(K - \frac{2G}{3}\right)\delta_{ij}\delta_{kl} - 2G\delta_{ik}\delta_{jl}$$

$$-\frac{\partial \bar{\chi}_{ij}}{\partial \alpha_{kl}} = \frac{\partial^2 f}{\partial \alpha_{ij}\alpha_{kl}} \tag{C6}$$

$$= \left(K - \frac{2G}{3}\right)\delta_{ij}\delta_{kl} + 2G\delta_{ik}\delta_{jl}$$

$$\dot{\alpha}_{ij} = \lambda \frac{\partial y}{\partial \chi_{ij}} \tag{C7}$$

$$\frac{\partial y}{\partial \chi_{ij}} = \sum_{l=1}^{m}\left(\frac{\exp(bf_l)}{\sum_{k=1}^{n}\exp(bf_k)}\right)\frac{\partial f_l}{\partial \chi_{ij}} \tag{C8}$$

where

$$f_1 = \frac{(\chi_1 - \chi_2)}{2} - c \tag{C9}$$

$$f_2 = \frac{(\chi_2 - \chi_3)}{2} - c$$

$$f_3 = \frac{(\chi_3 - \chi_1)}{2} - c$$

$$f_4 = -\frac{(\chi_1 - \chi_2)}{2} - c$$

$$f_5 = -\frac{(\chi_2 - \chi_3)}{2} - c$$

$$f_6 = -\frac{(\chi_3 - \chi_1)}{2} - c$$

λ in Eq. C7 is obtained from the consistency conditions $\dot{y} = 0$ as follows:

$$\frac{\partial y}{\partial \sigma_{ij}}\dot{\sigma}_{ij} + \frac{\partial y}{\partial \alpha_{ij}}\dot{\alpha}_{ij} + \frac{\partial y}{\partial \chi_{ij}}\dot{\chi}_{ij} = 0 \tag{C10}$$

$$\frac{\partial y}{\partial \sigma_{ij}}\left(\frac{\partial \sigma_{ij}}{\partial \varepsilon_{kl}}\dot{\varepsilon}_{kl} + \frac{\partial \sigma_{ij}}{\partial \alpha_{kl}}\dot{\alpha}_{kl}\right) + \frac{\partial y}{\partial \alpha_{ij}}\left(\dot{\alpha}_{ij}\right) + \frac{\partial y}{\partial \chi_{ij}}\left(\frac{\partial \bar{\chi}_{ij}}{\partial \varepsilon_{kl}}\dot{\varepsilon}_{kl} + \frac{\partial \bar{\chi}_{ij}}{\partial \alpha_{kl}}\dot{\alpha}_{kl}\right) = 0$$

$$\left(\frac{\partial y}{\partial \sigma_{ij}}\frac{\partial \sigma_{ij}}{\partial \varepsilon_{kl}} + \frac{\partial y}{\partial \chi_{ij}}\frac{\partial \bar{\chi}_{ij}}{\partial \varepsilon_{kl}}\right)\dot{\varepsilon}_{kl} + \left(\frac{\partial y}{\partial \alpha_{kl}} + \frac{\partial y}{\partial \sigma_{ij}}\frac{\partial \sigma_{ij}}{\partial \alpha_{kl}} + \frac{\partial y}{\partial \chi_{ij}}\frac{\partial \bar{\chi}_{ij}}{\partial \alpha_{kl}}\right)\dot{\alpha}_{kl} = 0$$

$$\left(\frac{\partial y}{\partial \alpha_{kl}} + \frac{\partial y}{\partial \sigma_{ij}}\frac{\partial \sigma_{ij}}{\partial \alpha_{kl}} + \frac{\partial y}{\partial \chi_{ij}}\frac{\partial \bar{\chi}_{ij}}{\partial \alpha_{kl}}\right)\lambda\frac{\partial y}{\partial \chi_{kl}} = -\left(\frac{\partial y}{\partial \sigma_{ij}}\frac{\partial \sigma_{ij}}{\partial \varepsilon_{kl}} + \frac{\partial y}{\partial \chi_{ij}}\frac{\partial \bar{\chi}_{ij}}{\partial \varepsilon_{kl}}\right)\dot{\varepsilon}_{kl}$$

$$\lambda = \frac{-\left(\frac{\partial y}{\partial \sigma_{ij}}\frac{\partial \sigma_{ij}}{\partial \varepsilon_{kl}} + \frac{\partial y}{\partial \chi_{ij}}\frac{\partial \bar{\chi}_{ij}}{\partial \varepsilon_{kl}}\right)\dot{\varepsilon}_{kl}}{\frac{\partial y}{\partial \chi_{kl}}\left(\frac{\partial y}{\partial \alpha_{kl}} + \frac{\partial y}{\partial \sigma_{ij}}\frac{\partial \sigma_{ij}}{\partial \alpha_{kl}} + \frac{\partial y}{\partial \chi_{ij}}\frac{\partial \bar{\chi}_{ij}}{\partial \alpha_{kl}}\right)}$$

$$= \frac{-\left(\frac{\partial y}{\partial \chi_{ij}}\frac{\partial \bar{\chi}_{ij}}{\partial \varepsilon_{kl}}\right)\dot{\varepsilon}_{kl}}{\frac{\partial y}{\partial \chi_{kl}}\left(\frac{\partial y}{\partial \chi_{ij}}\frac{\partial \bar{\chi}_{ij}}{\partial \alpha_{kl}}\right)}$$

where $\frac{\partial y}{\partial \sigma_{ij}} = 0$ and $\frac{\partial y}{\partial \alpha_{ij}} = 0$. Note that the orthogonality postulate of Ziegler (1977) (i.e. $\chi_{ij} = \bar{\chi}_{ij}$) is used in Eq. C10.

The stresses can then be updated as follows:

$$\begin{Bmatrix} \dot{\sigma}_{ij} \\ -\dot{\vec{\chi}}_{ij} \end{Bmatrix} = \begin{bmatrix} \frac{\partial^2 f}{\partial \varepsilon_{ij}\varepsilon_{kl}} & \frac{\partial^2 f}{\partial \varepsilon_{ij}\alpha_{kl}} \\ \frac{\partial^2 f}{\partial \alpha_{ij}\varepsilon_{kl}} & \frac{\partial^2 f}{\partial \alpha_{ij}\alpha_{kl}} \end{bmatrix} \begin{Bmatrix} \dot{\varepsilon}_{kl} \\ \dot{\alpha}_{kl} \end{Bmatrix}$$

10 References

Abbo, A. J., and Sloan, S. W. (1995). A smooth hyperbolic approximation to the Mohr-Coulomb yield criterion. Computers and structures, 54(3), 427-441.

Abbo, A. J., Lyamin, A. V., Sloan, S. W., and Hambleton, J. P. (2011). A C2 continuous approximation to the Mohr–Coulomb yield surface. International Journal of solids and Structures, 48(21), 3001-3010.

Boyd, S., and Vandenberghe, L. (2004). Convex optimization. Cambridge university press.

Calafiore, G. C., and El Ghaoui, L. (2014). Optimization models. Cambridge university press. Cambridge.

Collins, I. F., and Houlsby, G. T. (1997). Application of thermomechanical principles to the modelling of geotechnical materials. Proceedings of the Royal Society of London. Series A: Mathematical, Physical and Engineering Sciences, 453(1964), 1975-2001.

Collins, I. F., and Kelly, P. A. (2002). A thermomechanical analysis of a family of soil models. Geotechnique, 52(7), 507-518.

Coombs, W. M., Crouch, R. S., and Augarde, C. E. (2010). Reuleaux plasticity: analytical backward Euler stress integration and consistent tangent. Computer Methods in Applied Mechanics and Engineering, 199(25-28), 1733-1743.

Coombs, W. M., and Crouch, R. S. (2011). Non-associated Reuleaux plasticity: analytical stress integration and consistent tangent for finite deformation mechanics. Computer methods in applied mechanics and engineering, 200(9-12), 1021-1037.

Coussy, O., Pereira, J. M., and Vaunat, J. (2010). Revisiting the thermodynamics of hardening plasticity for unsaturated soils. Computers and Geotechnics, 37(1-2), 207-215.

de Souza Neto, E. A., Perić, D., Owen, D. R. J. (2008). Computational methods for plasticity. John Wiley & Sons Ltd. Chichester, UK.

Germain, P., Suquet, P., and Nguyen, Q. S. (1983). Continuum thermodynamics. ASME Transactions Series E Journal of Applied Mechanics, 50, 1010-1020.

Houlsby, G. T., Amorosi, A., and Rojas, E. (2005). Elastic moduli of soils dependent on pressure: a hyperelastic formulation. Géotechnique, 55(5), 383-392.

Houlsby, G.T., Puzrin, A.M., 2000. A thermomechanical framework for constitutive models for rate-independent dissipative materials. Int. J. Plast. 16 (9), 1017–1047. doi: 10.1016/S0749-6419(99)0 0 073-X .

Houlsby, G. T., and Puzrin, A. M. (2006). Principles of hyperplasticity: an approach to plasticity theory based on thermodynamic principles. Springer Science and Business Media.

Houlsby, G. T., Abadie, C. N., Beuckelaers, W. J. A. P., and Byrne, B. W. (2017). A model for nonlinear hysteretic and ratcheting behaviour. International Journal of Solids and Structures, 120, 67-80.

Houlsby, G. T., Amorosi, A., and Rollo, F. (2019). Non-linear anisotropic hyperelasticity for granular materials. Computers and Geotechnics, 115, 103167.

Lai, Y., Liao, M., and Hu, K. (2016). A constitutive model of frozen saline sandy soil based on energy dissipation theory. International Journal of Plasticity, 78, 84-113.

Lagioia, R., and Panteghini, A. (2016). On the existence of a unique class of yield and failure criteria comprising Tresca, von Mises, Drucker–Prager, Mohr–Coulomb, Galileo–Rankine, Matsuoka–Nakai and Lade–Duncan. Proceedings of the Royal Society A: Mathematical, Physical and Engineering Sciences, 472(2185), 20150713.

Lagioia, R., and Panteghini, A. (2019). The difficult challenge of modelling the non-linear elastic behaviour of soils within a theoretically sound framework. International Journal for Numerical and Analytical Methods in Geomechanics, 43(11), 1978-1994.

Lester, A. M., and Sloan, S. W. (2018). A smooth hyperbolic approximation to the Generalised Classical yield function, including a true inner rounding of the Mohr-Coulomb deviatoric section. Computers and Geotechnics, 104, 331-357.

Li, X. S. (2007). Thermodynamics-based constitutive framework for unsaturated soils. 1: Theory. Géotechnique, 57(5), 411-422.

Moreau, J. J. (1970). Sur les lois de frottement, de viscosité et de plasticité. Comptes Rendus Acad. Sci. 271, 608-611, Paris (in French).

Ottosen, N. S., and Ristinmaa, M. (2005). The mechanics of constitutive modeling. Elsevier.

Panteghini, A., and Lagioia, R. (2014). A fully convex reformulation of the original Matsuoka–Nakai failure criterion and its implicit numerically efficient integration algorithm. International Journal for Numerical and Analytical Methods in Geomechanics, 38(6), 593-614.

Panteghini, A., and Lagioia, R. (2018). An approach for providing quasi-convexity to yield functions and a generalized implicit integration scheme for isotropic constitutive models based on 2 unknowns. International Journal for Numerical and Analytical Methods in Geomechanics, 42(6), 829-855.

Panteghini, A., and Lagioia, R. (2019). DISCUSSION: A smooth hyperbolic approximation to the generalised Classical yield function, including a true inner rounding of the Mohr-Coulomb deviatoric section by Alexander M. Lester and Scott W. Sloan. Computers and Geotechnics, 106, 347-349.

Sheng, D., Sloan, S. W., and Gens, A. (2004). A constitutive model for unsaturated soils: thermomechanical and computational aspects. Computational Mechanics, 33(6), 453-465.

Sloan, S. W., and Booker, J. R. (1986). Removal of singularities in Tresca and Mohr–Coulomb yield functions. Communications in Applied Numerical Methods, 2(2), 173-179.

Soare, S. C., and Benzerga, A. A. (2016). On the modeling of asymmetric yield functions. International Journal of Solids and Structures, 80, 486-500.

Suquet, P. (1982) Plasticité et homogénésation (in french), Ph.D. thesis, Univ. Pierre et Marie Curie, Paris.

Suryasentana, S. K., Burd, H. J., Byrne, B. W., and Shonberg, A. (2020). A systematic framework for formulating convex failure envelopes in multiple loading dimensions. Géotechnique, 70(4), 343-353.

Suryasentana, S. K., Burd, H. J., Byrne, B. W., & Shonberg, A. (2021). Automated procedure to derive convex failure envelope formulations for circular surface foundations under six degrees of freedom loading. Computers and Geotechnics, 104174.

Tengattini, A., Das, A., and Einav, I. (2016). A constitutive modelling framework predicting critical state in sand undergoing crushing and dilation. Géotechnique, 66(9), 695-710.

Zhang, Z., Chen, Y., and Huang, Z. (2018). A novel constitutive model for geomaterials in hyperplasticity. Computers and Geotechnics, 98, 102-113.

Ziegler, H. (1977) An introduction to thermomechanics, North Holland, Amsterdam (2nd ed. 1983)

11 Tables

Table 1: List of common convex base functions that are useful for constructing constitutive models. Here, a_{ij} may refer to strain ε_{ij}, true stress σ_{ij} or generalised stress χ_{ij}, and $a'_{ij} = a_{ij} - \frac{1}{3}a_{kk}\delta_{ij}$ is the deviatoric component. f_i is any convex function, θ is the Lode angle, x or x_i is any scalar. Note that due to CMM Rule 2c, if a function is convex in a'_{ij}, it is also convex in a_{ij}.

Name	Convex function
1st stress invariant[1]	$I_1(a_{ij}) = a_{ii}$
Mean stress[1]	$p = \frac{1}{3}I_1(a_{ij})$
Square root of 2nd deviatoric stress invariant (or 1/√2 of the Frobenius norm of deviatoric stress)[2]	$\sqrt{J_2(a_{ij})} = \sqrt{\frac{1}{2}a'_{ij}a'_{ji}}$
2nd deviatoric stress invariant[3]	$J_2(a_{ij}) = \frac{1}{2}a'_{ij}a'_{ji}$
Triaxial deviatoric stress	$q = \sqrt{3J_2(a_{ij})}$
Square of 1st stress invariant[4]	$I_1^2(a_{ij}) = a_{ii}a_{jj}$
Exponential	$\exp(kx)$ for any $k \in \mathbb{R}$
Powers of absolute value	$\lvert x\rvert^k$ for $k \geq 1$
Modified LogSumExp	$\mathrm{MLSE}(b, f_1, \ldots, f_n) = \frac{1}{b}\mathrm{LSE}(bf_1, \ldots, bf_n)$ where $\mathrm{LSE}(x_1, \ldots, x_n) = \log\left(\sum_{i=1}^{n}\exp(x_i)\right)$
Deviatoric shape function[5]	$J_\theta(a_{ij}) = \sqrt{J_2(a_{ij})}f_{\mathrm{shape}}(\theta(a_{ij}))$

[1] These are linear functions, which are both convex and concave.

[2] Every norm is a convex function.

[3] The square of a convex non-negative function is convex.

[4] The Hessian can be calculated as $H_{ijkl} = 2\delta_{ij}\delta_{kl}$ where δ is the Kronecker delta. From Eq. A3 in Appendix A, it can be shown that the Hessian is positive semidefinite since $y_{ji}H_{ijkl}y_{kl} = y_{ji}2\delta_{ij}\delta_{kl}y_{kl} = 2y_{jj}y_{kk} \geq 0$. Hence, the function is convex.

[5] This has only be shown to be convex heuristically, not analytically.

12 Figures

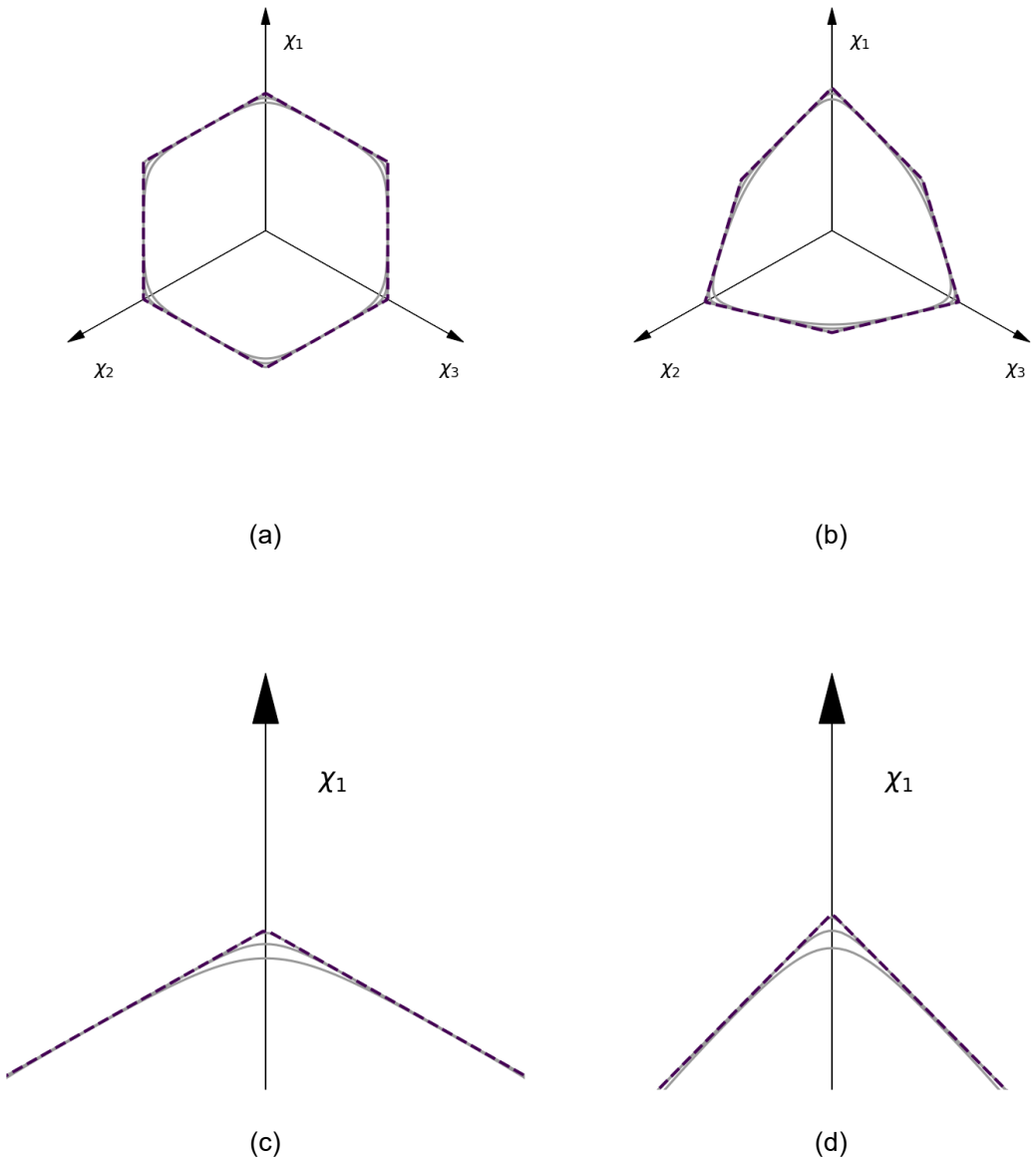

Figure 1: MLSE smooth approximations of the (a) Tresca and (b) Mohr Coulomb ($\phi = 30^o$) yield criterion in the deviatoric plane. Zoomed in versions of (a) and (b) are shown in (c) and (d) respectively, which highlights how close the MLSE smooth approximation is to the original criterion. The black dashed lines are the original non-smooth yield criteria, while the grey solid lines are the MLSE smooth approximations based on 3 b values ($10/c, 20/c, 100/c$ where c is the cohesive strength). The larger b is, the closer the MLSE smooth approximation is to the original criterion.

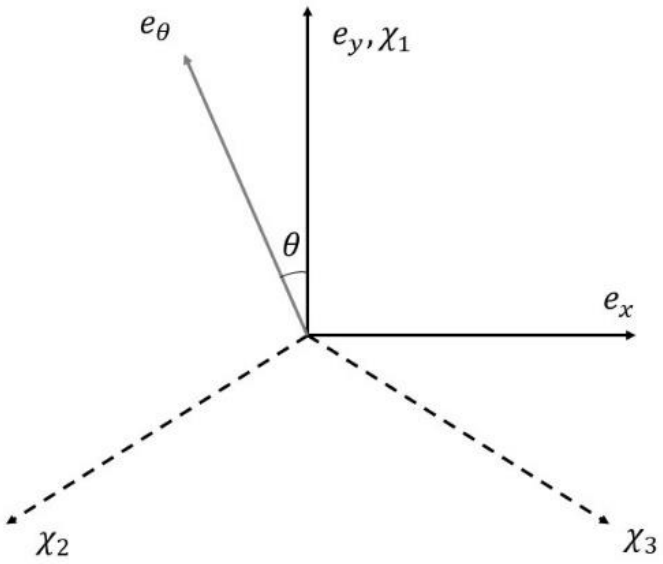

Figure 2: Schematic diagram of a generalised vector e_θ that points in any arbitrary direction along the deviatoric plane, where θ is the Lode angle.

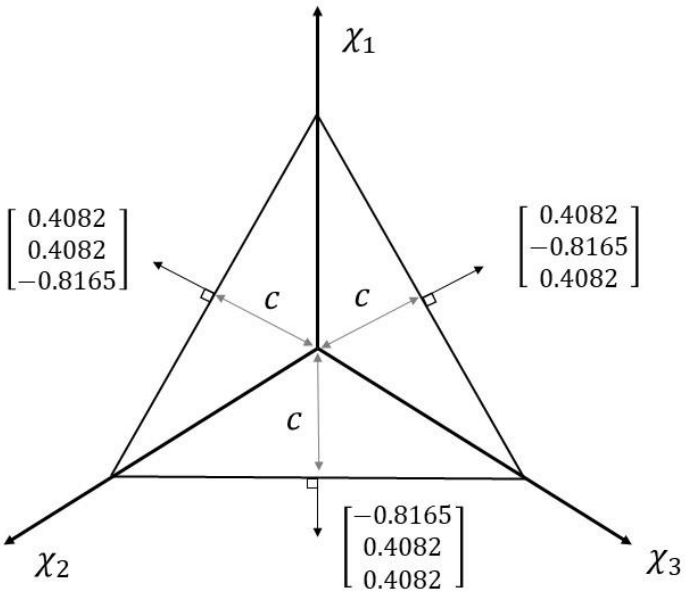

Figure 3: Schematic diagram showing the normal vectors of the hyperplanes that define the 3-sided polygonal yield surface in Eq. 24. Each hyperplane has a projected normal distance of c from the origin of the stress space.

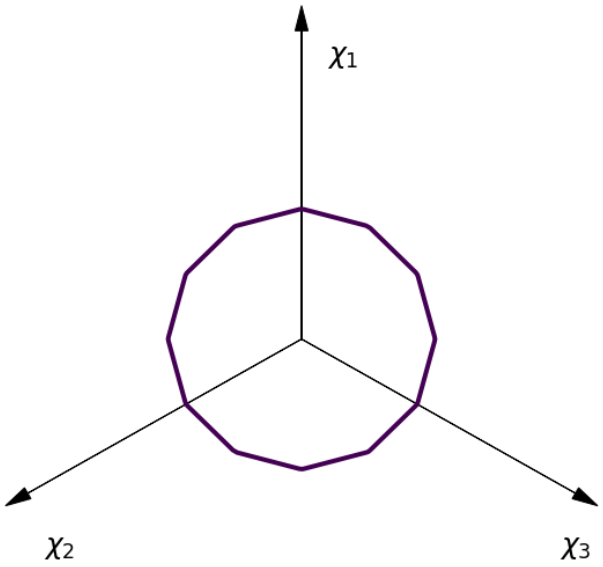

Figure 4: 12-sided polygonal yield surface in deviatoric plane

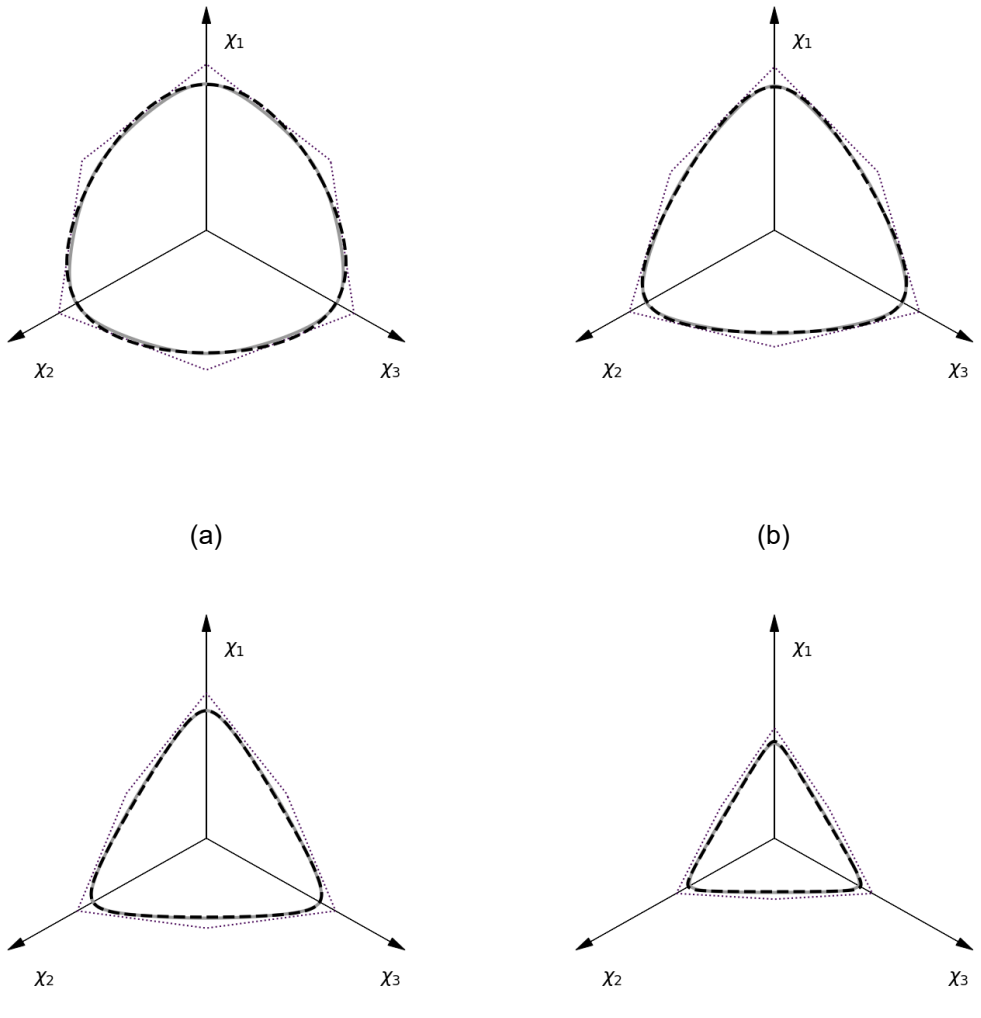

Figure 5: Original Matsuoka-Nakai yield function (black dashed line) and a convex and smooth approximation of the Matsuoka-Nakai yield function (grey solid line) in the deviatoric plane for (a) $\phi = \frac{\pi}{12}$ (b) $\phi = \frac{\pi}{6}$ (c) $= \frac{\pi}{4}$ (d) $\phi = \frac{\pi}{3}$. These lines virtually overlap each other. The black dotted line is the 'bounding support function' for the convex and smooth approximation of the Matsuoka-Nakai yield function.

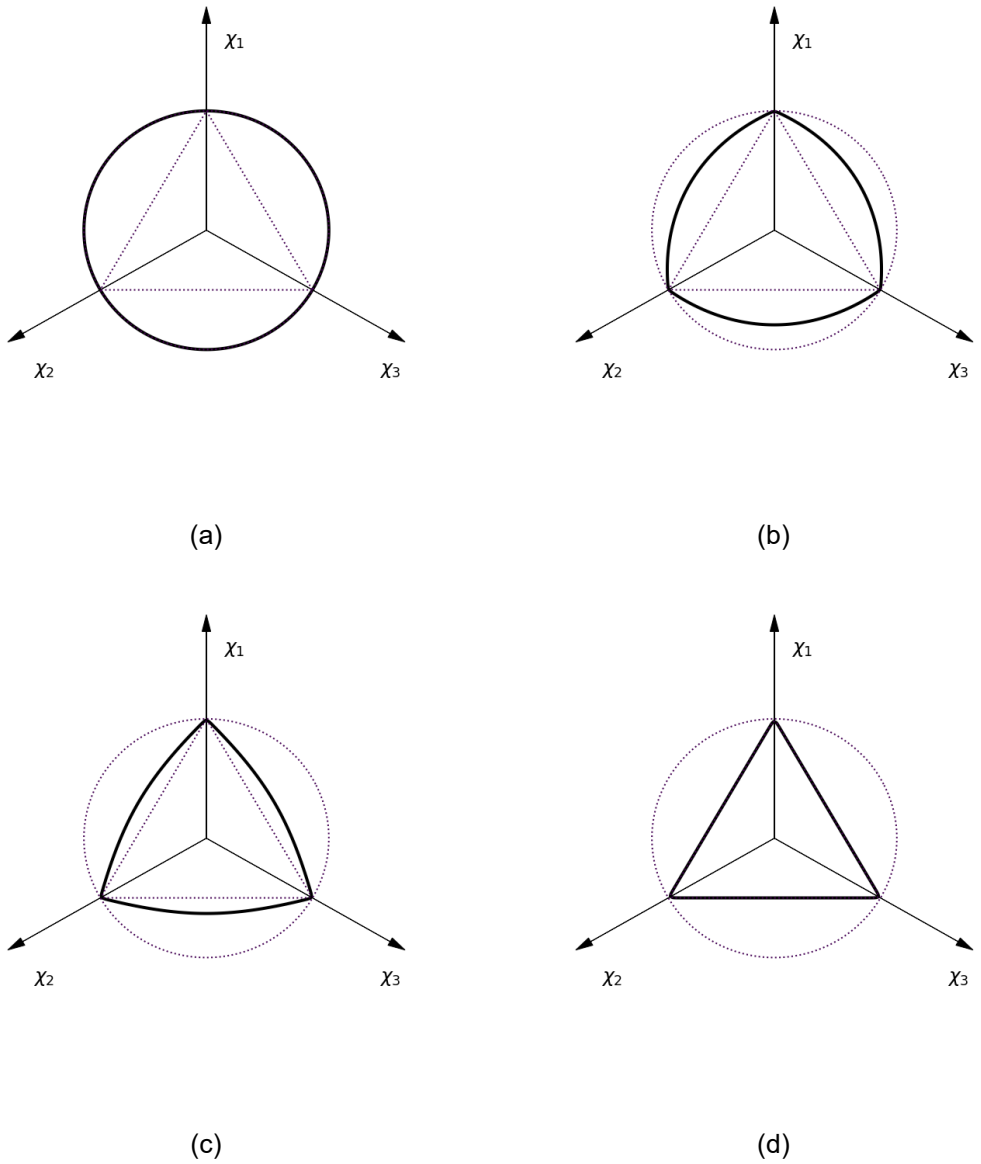

Figure 6: The convex and smooth ‘Reuleaux triangle’-shaped yield function defined by Eq. 30 in the deviatoric plane (shown in black solid line) for (a) $w = 0$ (b) $w = \frac{1}{3}$ (c) $w = \frac{2}{3}$ (d) $w = 1$. The black dotted lines are the components of the convex combination in Eq. 28.

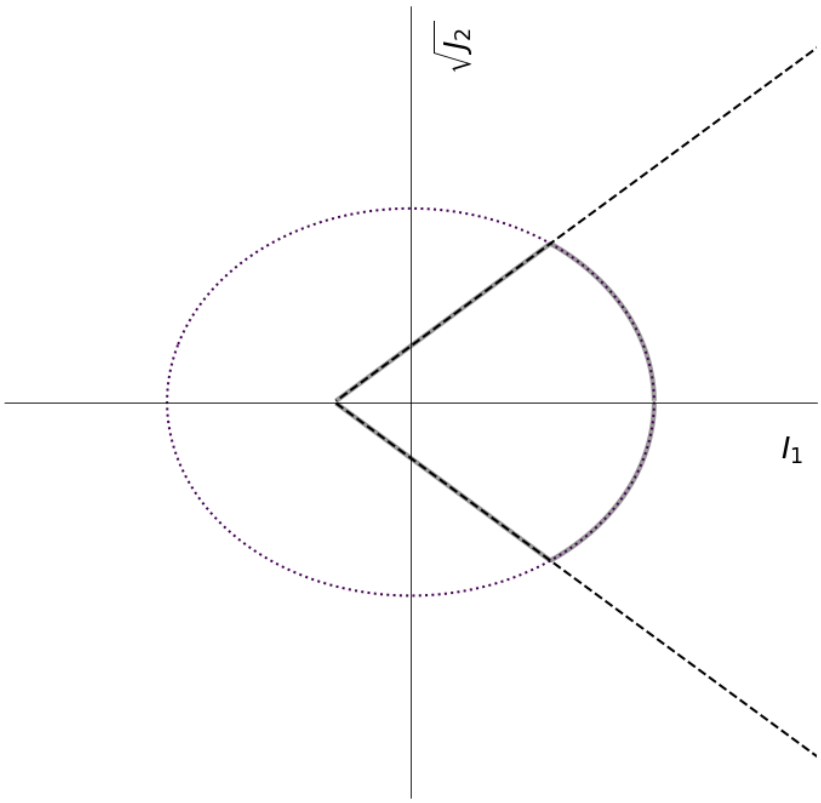

Figure 7: Yield surface (grey solid line) of the capped model y_{capped} in the meridional plane, where the black dashed line is the yield surface of the uncapped model y_{uncapped} and the black dotted line is the yield surface of the elliptical compressive cap $y_{\mathrm{cap\_c}}$.

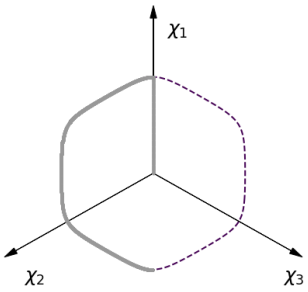

(a)

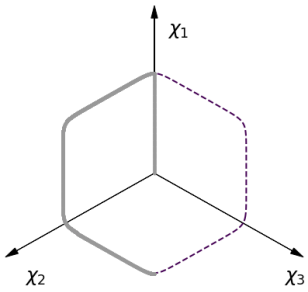

(b)

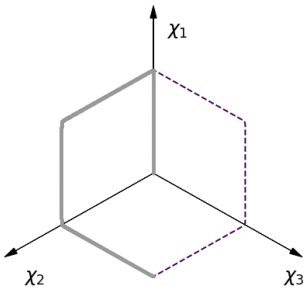

(c)

Figure 8: An element with the smooth MLSE-based Tresca yield function (Eq. 23) undergoing a strain-controlled stress path (shown in grey solid line) from the origin of the stress path to the yield surface (shown in black dashed line), and then travelling along the yield surface. Three smoothening b values were implemented: (a) $b = 10/c$; (b) $20/c$, and (c) $100/c$.

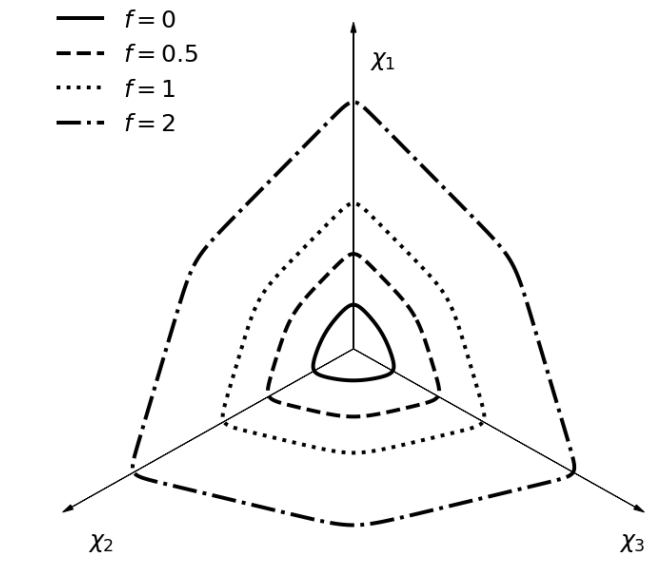

(a)

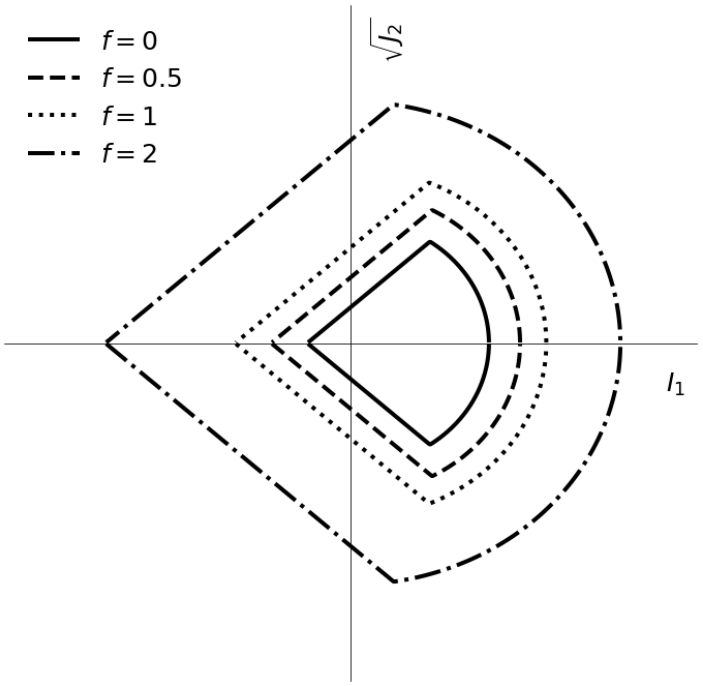

(b)

Figure 9: Yield surfaces in the inadmissible stress space (i.e. $f > 0$) for (a) the convex and smooth approximation of the Matsuoka-Nakai yield function (Eq. 26) in the deviatoric plane for $\phi = \frac{\pi}{6}$; (b) the capped yield function (Eq. 30) in the meridional plane.